Mechanics Research Communications 156 (2026) 104772

Contents lists available at ScienceDirect

Mechanics Research Communications

journal homepage: www.elsevier.com/locate/mechrescom

Vibration analysis of Bishop nanorods under transverse magnetic field effect

Aleyna Yazıcıoğlu [a], Ömer Civalek [a,b,*]

[a] Civil Engineering Department Division of Mechanics, Akdeniz University, 07070, Antalya, Turkey
[b] Department of Medical Research, China Medical University Hospital, China Medical University, Taichung, Taiwan

ARTICLE INFO

Keywords:
Magnetic field
Bishop rod theory
Nonlocal elasticity
Nanorods

ABSTRACT

This study presents the first analytical investigation of longitudinal vibration characteristics of Bishop-type nanorods subjected to transverse magnetic field. Two different boundary conditions are considered in the analysis: both clamped-clamped and clamped-free. In the Bishop nanorod model, shear deformation and rotational inertia effects are considered, and governing equation of motion of the system is formulated based on Hamilton's principle. Then, the electromechanical interaction terms generated by the transverse magnetic field are obtained based on Maxwell's equations, and these effects are integrated into equation of motion. The obtained governing differential equation is solved through suitable analytical transformations, and two distinct boundary conditions are taken into consideration. To demonstrate consistency of the model, the results obtained are compared with existing studies in literature. In addition, the effects of magnetic field parameters and nonlocal parameters on the natural frequency are investigated with a detailed parametric analysis. The study reveals opposing effects of magnetic field and size on nanoscale structures, providing theoretical basis for design of magneto-elastic nano sensors and NEMS-based devices.

1. Introduction

Nanotechnology is a research field concerned with the manipulation and structural control of matter at the nanoscale. Materials at these small dimensions, at dimensions of approximately 10^{-9} meters, exhibit various superior properties due to factors such as quantum effects and increased surface-to-volume ratios, differing from classical behavior observed at macroscopic levels. These properties enable their use in fields such as electronics [1,2], energy [3], defense [4], medicine [5], and engineering [6]. Their high performance, lightness, and strength open the door to innovative solutions. For these reasons, it has emerged as a rapidly developing research field in recent years.

Results obtained from experimental analyses and molecular dynamics simulations indicate that classical continuum theories are not adequate describing mechanical behavior of nanoscale materials. However, experimental methods and atomistic/molecular-based simulations require high time costs and significant computational power. The complexity of the problem increases, especially as the geometric properties, boundary conditions, and material types of the system vary, this further limit the applicability and efficiency of these methods. Due to these disadvantages, researchers have proposed improved continuum theories that can account for nanoscale effects and have focused on obtaining more efficient solutions through analytical methods. These theories are commonly referred to in literature as higher-order elasticity theories. Prominent examples include nonlocal elasticity theory [7,8], modified couple stress theory [9], modified strain gradient theory [10], surface elasticity theory [11], doublet mechanics [12] and nonlocal strain gradient theory [13] Among these approaches, Eringen's nonlocal elasticity theory has become one of the most widely used frameworks for modeling the size-dependent behavior of nanostructures. This theory is available in both differential and integral forms. Although the differential nonlocal model (NDM) offers significant mathematical convenience and provides analytical solutions in closed form, some studies have reported paradoxical responses and inconsistencies related to boundary conditions in certain nanoscale problems [14,15]. To overcome these limitations, nonlocal integral formulations have been developed, and it has been demonstrated that these formulations provide mathematically well-defined descriptions of nanostructures while preventing some of the paradoxes observed in differential formulations [16–19]. However, due to its analytical tractability and widespread use in the vibration and stability analysis of nanoscale structures, the differential form of Eringen's nonlocal elasticity theory continues to be

* Corresponding author at: Civil Engineering Department Division of Mechanics, Akdeniz University, 07070, Antalya, Turkey.
E-mail addresses: aleynayazicioglu@akdeniz.edu.tr (A. Yazıcıoğlu), civalek@yahoo.com (Ö. Civalek).

https://doi.org/10.1016/j.mechrescom.2026.104772
Received 11 April 2026; Received in revised form 15 June 2026; Accepted 19 July 2026
Available online 20 July 2026
0093-6413/© 2026 Elsevier Ltd. All rights are reserved, including those for text and data mining, AI training, and similar technologies.

widely used in the literature and has therefore been adopted in the present study. In general, higher-order continuum theories have provided an efficient framework for capturing size-dependent effects at the nanoscale, thereby overcoming many of the limitations of classical continuum models while reducing the computational burden associated with experimental and molecular dynamics approaches.

For instance, one of the pioneering works towards applying nonlocal elasticity theory to nanoscale structures developed a nonlocal formulation of Bernoulli/ Euler beam theory [20]. The equations of motion for various beam theories, including Euler–Bernoulli, Timoshenko, Reddy, and Levinson beam models, were reformulated within the framework of Eringen's nonlocal elasticity theory. These formulations enabled the analysis of bending, vibration, and buckling behaviors while accounting for size-dependent effects at micro- and nano-scales [21]. Similar problems were investigated in another study within the framework of nonlocal shear deformation beam theory [22]. The bending behavior of nano and micro-scale beams under concentrated and distributed loads was investigated using a nonlocal Euler–Bernoulli beam model [23]. The stability problem of a micro-scale beam was analytically investigated using advanced elasticity theories, including strain gradient elasticity theory and the modified couple stress model [24]. Another study examined the influence of nonlocal effects on the dynamic behavior of nanoscale system and proposed nonlocal finite element approach to analyze axial vibrations of nanorods, flexural vibrations of nanobeams, and transverse vibrations of nanoplates [25]. A similar solution method was used to perform a free vibration analysis of a functionally graded (FG) nanobeam [26]. The thermal buckling and vibration behavior of temperature-dependent FG Timoshenko nanobeams under in-plane thermal loading were investigated using analytical Navier-type solutions formulated within Eringen's nonlocal elasticity framework [27].A revised formulation of the Timoshenko beam theory was introduced, leading to a simpler and more consistent governing differential equation; asymptotic basis of the proposed equation and its boundary/initial conditions were thoroughly examined [28]. An extended formulation of Eringen's nonlocal elasticity model incorporating gradient effects was proposed to investigate small-scale effects in nanorods with FG Young's modulus along the cross-section. Equilibrium equations were obtained using a variational approach and closed-form analytical solutions of axial displacements field and corresponding forces were presented for cantilevers and clamped-clamped boundary conditions [29]. The longitudinal forced vibration behavior of the nanorod was investigated under constant, linear, and sinusoidal loading conditions; the obtained results were presented comparatively with classical elasticity theory [30]. The longitudinal free vibration behavior of thick nanorods with homogeneous and axially functionally graded material properties has been investigated within the framework of Rayleigh–Bishop rod theory [31,32]. Wave propagation of nanorods was analyzed using Rayleigh-Bishop rod theory, which includes shear deformation and lateral inertia [33]. A novel nonlocal analytical formulation based on Bishop rod theory was developed to analyze the static response of porous, thick circular nanorods embedded in an elastic medium [34]. The literature contains numerous studies based on various rod theories that examine different effects [35–39].

Studies on nanoscale structures have become increasingly diverse; comprehensive research has been conducted taking into account different physical and geometric effects. For example, vibration of nanopeapod embedded in elastic medium and containing C_{60} molecules in bulk masses [40], static bending behavior of nanobeams under electrical loads such as flexoelectricity [41], torsional vibration of nanorods surrounding by elastic matrix [42], FG nanobeams under the influence of thermos-magnetic fields and moving loads [43], torsional response of nanorods made of auxetic honeycomb material [44], rotating nanobeams [45], nanoring embedded in elastic medium [46], dynamic vibration behavior of porous Bishop nanorods considering arbitrary boundary conditions [47], response exhibited by elliptical nanorod exposed to linear and nonlinear external torque [48], thermal vibration characteristics of cracked nanobeams resting on an elastic basis were performed [49] and work in this field continues today [50–53].

In addition to these studies, presence of a magnetic field is one of common physical interactions to which nanoscale systems are subjected. Therefore, influence of magnetic fields on behavior of nanomaterials has attracted considerable attention in recent studies. In one study, axial vibration in nanorod structures, such as carbon nanotubes (CNT), under transverse magnetic field was investigated based on nonlocal elasticity framework [54]. Axial free vibration characteristics of a complex multi-nanorod structure containing Lorentz magnetic force and consisting of m partial differential equations were investigated [55]. Kiani examined influence of magnetic fields on dynamic behavior of CNT in several studies, analyzing vibration and instability characteristics of single- and double-walled CNT under different magnetic field conditions [56–58]. Additionally, the wave propagation behavior in carbon nanotubes under influence of magnetic fields was also examined [59,60]. In another study, the dynamic response of a monolayer graphene sheet supported by a viscoelastic foundation subject to longitudinal magnetic field was investigated based on nonlocal sinusoidal shear deformation theory [61]. Vibration characteristics and thermal buckling response of FG porous nanobeams exposed to combined magnetic and thermal fields were investigated [62]. Furthermore, axial vibration behavior of short fiber-reinforced nanorods subjected to magnetic field and elastic medium was investigated within framework of nonlocal elasticity theory. Equation of motion was obtained by considering Lorentz magnetic force [63]. Nonlinear free vibration analysis of magneto-electro-elastic nanobeams was performed using a model combining nonlocal elasticity theory and modified couple stress theory [64]. A novel formulation based on nonlocal elasticity theory was developed for the free vibration analysis of magneto-electro-elastic (MEE) nanobeams resting on an elastic foundation [65].

As observed in the literature, although there are studies investigating vibration behavior of nanorods exposed to a magnetic field, these analyses have predominantly been based on classical rod formulations or beam theories. While Euler–Bernoulli and Timoshenko theories are widely employed for flexural vibration analyses, they are not specifically intended to account for the Poisson-induced transverse motion that accompanies axial deformation. In contrast, the Bishop rod model incorporates lateral inertia associated with transverse deformation as well as shear stiffness effects, providing a more comprehensive description of longitudinal vibration behavior. The accurate prediction of vibration characteristics is essential for the design of nanoscale resonators, sensors, actuators, and NEMS devices operating under electromagnetic environments. Since the performance of such systems is highly sensitive to both size-dependent effects and external magnetic fields, simplified rod models may not always provide sufficient accuracy. Therefore, there is a need for advanced formulations capable of simultaneously accounting for nonlocal effects, magnetic interactions, lateral inertia, and shear stiffness. This requirement motivates the present study.

Despite the growing interest in magneto-elastic nanostructures, no analytical study has yet examined the longitudinal vibration characteristics of Bishop-type nanorods subjected to a transverse magnetic field. Motivated by this gap, the present work investigates the dynamic behavior of nonlocal Bishop nanorods under magnetic field effects. To this end, the governing equation of motion, including lateral inertia, Poisson's ratio, and shear stiffness contributions, is first established within the framework of nonlocal elasticity theory. Subsequently, the magnetic field effect derived from Maxwell's equations is incorporated into the formulation through the Lorentz force. Using the resulting model, the influences of the magnetic parameter, magnetic field strength ratio, and nonlocal parameter on the dimensionless natural frequencies are systematically investigated for clamped–free and clamped–clamped boundary conditions.

The main contributions of this study can be summarized as follows:

- A nonlocal Bishop nanorod model exposed to a transverse magnetic field has been developed for the longitudinal vibration analysis of nanorods.
- The magnetic field-induced Lorentz force has been incorporated into the Bishop model's equation of motion within the framework of nonlocal elasticity theory.
- The combined effects of the nonlocal parameter, magnetic field parameter, and magnetic field strength ratio on nondimensional natural frequencies have been systematically investigated.
- A direct comparison between the classical nonlocal rod model and the nonlocal Bishop rod model has been presented, and the importance of lateral inertia and shear stiffness effects in magneto-elastic nanoscale structures has been revealed.
- New information has been provided regarding the dynamic behavior of nanorods operating in electromagnetic environments for different boundary conditions.

The results obtained show that there is an inverse interaction between the nonlocal parameter and the magnetic field parameter. Furthermore, significant differences in natural frequency values were observed between the Bishop nanorod model and the classical nanorod model. This situation demonstrates that the effects of lateral inertia and shear stiffness at the nanoscale in presence of magnetic field are significant to a degree that cannot be neglected.

2. Mathematical Formulations

2.1. Nonlocal Bishop Nanorod Model

During axial deformations, the cross-section of the nanorod exhibits a tendency to shrink or expand transversely due to the Poisson effect. In line with this physical phenomenon, this study investigates axial vibration behavior of the nanorod, considering not only axial displacement but also lateral inertial effects and shear stiffness contributions. In the context of the Bishop rod formulation, displacement field at arbitrary point within nanorod is expressed as follows [66]:

$$u = u(x,t),\ v = -\upsilon y\frac{\partial u(x,t)}{\partial x},\ w = -\upsilon z\frac{\partial u(x,t)}{\partial x} \tag{1}$$

here $u(x, t)$ represents axial displacement, whereas $v(x, y, t)$ and $w(x, y, t)$ represent transverse displacement of the nanorod. Additionally, υ is Poisson's ratio. According to Bishop rod model, the nonzero strain components are written as follows:

$$\varepsilon_{xx} = \frac{\partial u}{\partial x},\ \varepsilon_{yy} = \frac{\partial v}{\partial y} = -\upsilon\frac{\partial u(x,t)}{\partial x},\ \varepsilon_{zz} = \frac{\partial w}{\partial z} = -\upsilon\frac{\partial u(x,t)}{\partial x} \tag{2}$$

$$\gamma_{xy} = \frac{\partial u}{\partial y}+\frac{\partial v}{\partial x} = -\upsilon y\frac{\partial^2 u(x,t)}{\partial x^2},\ \gamma_{xz} = \frac{\partial u}{\partial z}+\frac{\partial w}{\partial x} = -\upsilon z\frac{\partial^2 u(x,t)}{\partial x^2},\ \gamma_{yz} = \frac{\partial v}{\partial z}+\frac{\partial w}{\partial y} = 0$$

Here, ε and γ denote the normal and shear strains, respectively.

Classical (local) elasticity theories are incapable of accurately capturing the size-dependent effects that become prominent at the nanoscale; consequently, nonlocal elasticity theories have been developed to overcome this limitation. Among these, the nonlocal elasticity theory proposed by Eringen [7] assumes that the stress at a given point is influenced not only by the strain at that point but also by the strain field in its surrounding domain. Accordingly, the nonlocal linear constitutive relation is expressed as:

$$\sigma_{ij}(x) = \int \alpha(|x-x'|,\ \tau)t_{ij}(x')dV(x'),\ \forall x\ \epsilon\ V \tag{3a}$$

$$\sigma_{ij} = \rho\left(\ddot{u}_j - f_j\right) \tag{3b}$$

$$\varepsilon_{ij}(x') = \frac{1}{2}\left(u_{i,j}+u_{j,i}\right) \tag{3c}$$

$$t_{ij}(x') = \lambda\varepsilon_{rr}\delta_{ij}+2\widetilde{\mu}\varepsilon_{ij}(x') \tag{3d}$$

Here; σ_{ij} refer to the stress tensor, while $\alpha(|x - x'|, \tau)$ denotes nonlocal kernel function, where $|x - x'|$ indicates Euclidean distance between two points. The parameter $\tau = e_0a/l$, where e_0,a and l denotes material-related coefficient, internal and external characteristic length parameters of material, respectively. $t_{ij}(x')$ and $\varepsilon_{ij}(x')$ local stress and strain tensor at arbitrary point x' in body. V represents volume of material, ρ represents the material density and f_i denotes the body force. δ_{ij} denotes Kronecker delta function and lastly λ and $\widetilde{\mu}$ is Lame constant. Furthermore, Eringen [7] proposed the following the constitutive relation for nonlocal elasticity in differential form for ease of processing:

$$\left(1-\mu^2\nabla^2\right)\sigma_{ij} = t_{ij} = \lambda\varepsilon_{rr}\delta_{ij}+2\widetilde{\mu}\varepsilon_{ij}(x') \tag{4}$$

Here, $\nabla^2 = \frac{\partial^2}{dx^2}+\frac{\partial^2}{dy^2}+\frac{\partial^2}{dz^2}$ refer to the Laplace operator, and the parameter $\mu = e_0a$ represents the nonlocal parameter characterizing the small-scale effects in Eringen's nonlocal elasticity theory. In this expression, a describes internal characteristic length (lattice parameter, granular size and distance between C–C bonds) and e_0 is a constant appropriate to each material that can be identified from atomistic simulations or by using the dispersive curve of the Born–Karman model of lattice dynamics [66]. In literature, the nonlocal parameter is generally treated either in a dimensional form in the range of 0-2 nm or in a nondimensional form normalized to the external characteristic length (μ/L) of the structure. Both approaches are widely used to study small-scale effects in nanostructures. In this study, results are presented using both representations to facilitate comparison with existing studies and to demonstrate the effect of the nonlocal effect from different perspectives. It should also be noted that when $\mu = 0$ (or equivalently $(\mu/L = 0)$, the nonlocal formulation is reduced to the corresponding classical local rod theory, indicating the absence of small-scale effects.

Using Eq. (2) and Eq. (4), the nonlocal constitutive relation for the Bishop nanorod, which also considers the effects of lateral motion and shear stiffness, is expressed as follows [66]:

$$\sigma_{xx}-\mu^2\frac{\partial^2\sigma_{xx}}{\partial x^2} = E\frac{\partial u}{\partial x} \tag{5a}$$

$$\sigma_{xy}-\mu^2\frac{\partial^2\sigma_{xy}}{\partial x^2} = -G\upsilon y\frac{\partial^2 u(x,\ t)}{\partial x^2} \tag{5b}$$

$$\sigma_{xz}-\mu^2\frac{\partial^2\sigma_{xz}}{\partial x^2} = -G\upsilon z\frac{\partial^2 u(x,\ t)}{\partial x^2} \tag{5c}$$

In the Eq. (5), E and G stand for elastic modulus and shear modulus, respectively. Additionally, using Eq. (3b) and (5), system of equations can be expressed as:

$$\frac{\partial\sigma_{xx}}{\partial x}+\frac{\partial\sigma_{xy}}{\partial y}+\frac{\partial\sigma_{xz}}{\partial z} = \rho\left(\frac{\partial^2 u}{\partial t^2}-\widetilde{f_x}\right) \tag{6a}$$

$$\frac{\partial\sigma_{xy}}{\partial x} = \rho\left(\frac{\partial^2 v}{\partial t^2}-\widetilde{f_y}\right) \tag{6b}$$

$$\frac{\partial\sigma_{xz}}{\partial x} = \rho\left(\frac{\partial^2 w}{\partial t^2}-\widetilde{f_z}\right) \tag{6c}$$

In the Eq. (6), $\rho\frac{\partial^2 u}{\partial t^2}$, $\rho\frac{\partial^2 v}{\partial t^2}$, $\rho\frac{\partial^2 w}{\partial t^2}$ are inertia forces and $\rho\widetilde{f_x}$, $\rho\widetilde{f_y}$, $\rho\widetilde{f_z}$ represent body force densities along the x, y and z directions, respectively. By substituting Eq. (1) into Eq. (6) and neglecting body force densities $\widetilde{f_y}$ and $\widetilde{f_z}$ and then inserting the resulting expressions into Eq. (5), the stress components σ_{xx}, σ_{xy}, and σ_{xz} can be formulated using the displacement u as follows:

$$\sigma_{xx} = \mu^2 \frac{\partial}{\partial x}\left[(1+2\upsilon)\rho\frac{\partial^2 u}{\partial t^2} - \rho\tilde{f}_x\right] + E\frac{\partial u}{\partial x} \tag{7a}$$

$$\sigma_{xy} = -\mu^2\rho\upsilon y\frac{\partial^4 u(x,t)}{\partial x^2\partial t^2} - G\upsilon y\frac{\partial^2 u(x,\ t)}{\partial x^2} \tag{7b}$$

$$\sigma_{xz} = -\mu^2\rho\upsilon z\frac{\partial^4 u(x,t)}{\partial x^2\partial t^2} - G\upsilon z\frac{\partial^2 u(x,\ t)}{\partial x^2} \tag{7c}$$

By applying Hamilton's principle, equations of motion corresponding to nonlocal Bishop rod formulation are derived [67]:

$$\delta\int_{t_1}^{t_2}(K-\Pi+W)dt = 0 \tag{8}$$

In the above equations, $t_1 < t < t_2$ denotes the time interval, while K, Π and W represent to kinetic energy, strain energy and external work, respectively. The kinetic energy term is expressed as:

$$K = \frac{1}{2}\int_A\int_0^L \rho\left[\left(\frac{\partial u}{\partial t}\right)^2 + \left(\frac{\partial v}{\partial t}\right)^2 + \left(\frac{\partial w}{\partial t}\right)^2\right]dxdA$$
$$= \frac{1}{2}\int_0^L \rho A\left[\left(\frac{\partial u}{\partial t}\right)^2 + \rho I_p\upsilon^2\left(\frac{\partial^2 u}{\partial t\,\partial x}\right)^2\right]dx \tag{9}$$

Here, L denotes the length of the nanorod, I_p is polar moment of inertia of Bishop nanorod, and A denotes cross-sectional area. These quantities are given by:

$$A = \int_A dA,\ I_p = \int_A (y^2+z^2)dA \tag{10}$$

Strain energy of nanorod is given by:

$$\Pi = \frac{1}{2}\int_A\int_0^L \sigma_{xx}\varepsilon_{xx} + \sigma_{xy}\gamma_{xy} + \sigma_{xz}\gamma_{xz})dxdA = \frac{1}{2}\int_0^L\left(N_x\frac{\partial u}{\partial x} - \upsilon P_x\frac{\partial^2 u}{\partial x^2}\right)dx \tag{11}$$

where N_x and P_x indicate the stress resultants, which take the following form:

$$N_x = \int_A \sigma_{xx}\ dA,\ P_x = \int_A (\sigma_{xy}y + \sigma_{xz}z)dA \tag{12}$$

External work is defined as:

$$W = \int_0^L f(x,t)\ udx \tag{13}$$

Here, $f(x,\ t)$ denotes axial force induced by applied magnetic field. When the kinetic energy expression obtained in Eq. (9), the strain energy given in Eq. (11), and external work term defined in Eq. (13) are substituted into Eq. (8), which expresses Hamilton's principle, following expression is obtained for the displacement field δu:

$$\delta u:\ \frac{\partial N_x}{\partial x} + \upsilon\frac{\partial^2 P_x}{\partial x^2} + f(x,t) - \rho A\frac{\partial^2 u}{\partial t^2} - \rho I_p\upsilon^2\frac{\partial^4 u}{\partial x^2\partial t^2} \tag{14}$$

and the boundary conditions associated with nonlocal Bishop nanorod formulation can be expressed as:

$$\left(N_x + \upsilon\frac{\partial P_x}{\partial x} + \rho I_p\upsilon^2\frac{\partial^4 u}{\partial x^2\partial t^2}\right)\delta u\Big|_0^L = 0$$

$$(\upsilon P_x)\delta\frac{\partial u}{\partial x}\Big|_0^L = 0 \tag{15}$$

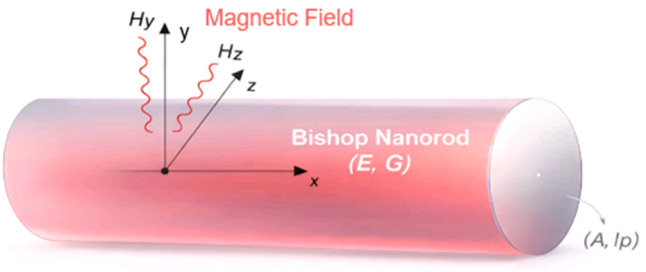


Fig. 1. Bishop nanorod under transverse magnetic field effect.

Using Eq. (7) in Eq. (12), the stress resultants corresponding to the nonlocal Bishop nanorod are derived as:

$$N_x = \mu^2\rho A(1+2\upsilon)\frac{\partial^3 u}{\partial x\ \partial t^2} + EA\frac{\partial u}{\partial x} - \mu^2\frac{\partial f(x,t)}{\partial x} \tag{16a}$$

$$P_x = -G\upsilon I_p\frac{\partial^2 u}{\partial x^2} - \mu^2 I_p\rho\upsilon\frac{\partial^4 u}{\partial x^2\partial t^2} \tag{16b}$$

In the formulation of above expressions, the force term is $\tilde{f}_x = \frac{f(x,\ t)}{\rho A}$. As a result, By inserting Eq. (16) into Eq. (14), the governing equation of motion of Bishop nanorod model can be obtained in terms of the axial displacement $u(x,\ t)$:

$$\rho A\frac{\partial^2 u}{\partial t^2} - \rho I_p\upsilon^2\frac{\partial^4 u}{\partial x^2\partial t^2} - f(x,t) - EA\frac{\partial^2 u}{\partial x^2} + GI_p\upsilon^2\frac{\partial^4 u}{\partial x^4}$$
$$= \mu^2\frac{\partial^2}{\partial x^2}\left[\rho A(1+2\upsilon)\frac{\partial^2 u}{\partial t^2} - \rho I_p\upsilon^2\frac{\partial^4 u}{\partial x^2\partial t^2} - f(x,t)\right] \tag{17}$$

2.2. Magnetic field formulation based on Maxwell's relations

This work aims to analyze axial vibration response of the Bishop nanorod subjected to magnetic field (see Fig. 1). When dealing with nanoscale structures, the effects of electromagnetic fields on mechanical behavior can be significant. Therefore, accurately modeling interaction between the magnetic field and mechanical deformation is critical for dynamic analysis. Within this scope, influence of magnetic field on the structure has been incorporated into model through the Lorentz magnetic force derived based on Maxwell's equations. Lorentz force defines interaction between the electromagnetic field and the conductive medium, contributing to the dynamic behavior of the structure along the axial direction as an additional loading term. Thus, an electromagnetic force component is added to system's equations of motion.

Maxwell's equations are the fundamental relationships that describe the basic interactions between electric and magnetic fields and form the basis of electromagnetic field theory. They are widely used in literature to model effect of magnetic fields on different structural elements and continuity models [61,62,68,69] In this study, influence of magnetic field on nanorod is described using Maxwell's equations, and the associated relations are presented as [54,69]:

$$\mathrm{J} = \nabla\ \times\ \mathrm{h} \tag{18a}$$

$$\nabla\ \times\ \mathrm{e} = -\eta\frac{\partial \mathrm{h}}{\partial x} \tag{18b}$$

$$\nabla\ .\ \mathrm{h} = 0 \tag{18c}$$

$$\mathrm{h} = \nabla\ \times\ (\mathrm{U}\ \times\ \mathrm{H}) \tag{18d}$$

$$\mathrm{e} = -\eta\left(\frac{\partial \mathrm{U}}{\partial t}\ \times\ \mathrm{H}\right) \tag{18e}$$

$$\mathrm{f}\left(f_x,\ f_y,\ f_z\right) = \eta\ (\mathrm{J}\ \times\ \mathrm{H}) \tag{18f}$$

Here, J, h, e, f and η represents the current density, magnetic field's distribution, electric fields strength vectors, Lorentz force and magnetic field permeability, respectively. In addition, ∇ denotes the Hamilton operator, defined as:

$$\nabla = \mathrm{i}\frac{\partial}{\partial x} + \mathrm{j}\frac{\partial}{\partial y} + \mathrm{k}\frac{\partial}{\partial z} \tag{19}$$

In the above equation, i, j and k denote unit vectors along x, y and z directions, respectively, which correspond to the length, width, and height coordinates of the material. Also, U represent the displacement vector, defined as:

$$\mathrm{U} = u(x,t)\ \mathrm{i} + v(x,t)\ \mathrm{j} + w(x,t)\ \mathrm{k} \tag{20}$$

here, $u(x,t)$, $v(x,t)$ and $w(x,t)$ denote the displacement components along the x, y and z directions, respectively. The transverse magnetic field vector is defined as $\mathrm{H} = (0,\ \mathrm{H_y},\ \mathrm{H_z})$, where $\mathrm{H_y}$ and $\mathrm{H_z}$ represent the magnetic field intensities in the y and z directions. In this study, the magnetic field is assumed to act orthogonally to the longitudinal axis of the nanorod, as shown in Fig. 1. As a result, the magnetic field vector is formulated as:

$$\mathrm{h} = 0\mathrm{i} + \mathrm{H_y}\frac{\partial \mathrm{u}}{\partial \mathrm{x}}\mathrm{j} - \mathrm{H_z}\frac{\partial \mathrm{u}}{\partial \mathrm{x}}\mathrm{k} \tag{21}$$

In the above equation, the displacement components $v(x,t)$ and $w(x,t)$ in the y and z directions are neglected. By substituting Eq. (21) into Eq. (18a), we obtain current density as:

$$\mathrm{J} = 0\mathrm{i} + \mathrm{H_z}\frac{\partial^2 u}{\partial x^2}\mathrm{j} - \mathrm{H_y}\frac{\partial^2 u}{\partial x^2}\mathrm{k} \tag{22}$$

Additionally, when Eq. (22) is added to the expression for Lorentz force induced by longitudinal magnetic field,

$$\mathrm{f}\left(f_x,\ f_y,\ f_z\right) = \eta\ (\ \mathrm{J}\ \times\ \mathrm{H}) = \ \eta\left[\left(H_y^2 + H_z^2\right)\frac{\partial^2 u}{\partial x^2}\mathrm{i} + 0\mathrm{j} + 0\mathrm{k}\right] \tag{23}$$

Now, considering both the axial displacement $u(x,t) = u$ and the Lorentz force in the x directions, this can be expressed as:

$$\mathrm{f}\ (f_x) = \ \eta\left[\left(H_y^2 + H_z^2\right)\frac{\partial^2 u}{\partial x^2}\mathrm{i}\right] \tag{24}$$

Finally, the force per unit length of nanorod $\left(\breve{\mathrm{f}}\right)$ is given by following expression [54,69]:

$$\breve{\mathrm{f}} = \int \mathrm{f}\ (f_x)\ dA = \ \eta A\left(H_y^2 + H_z^2\right)\frac{\partial^2 u}{\partial x^2} \tag{25}$$

When the axial magnetic force term obtained in the above equation is substituted into Eq. (17), the governing equation of motion for the Bishop nanorod under transverse magnetic field influence is obtained.

$$\begin{aligned}&\rho A\frac{\partial^2 u}{\partial t^2} - \rho I_p v^2\frac{\partial^4 u}{\partial x^2 \partial t^2} - \eta A\left(H_y^2 + H_z^2\right)\frac{\partial^2 u}{\partial x^2} - EA\frac{\partial^2 u}{\partial x^2} + GI_p v^2\frac{\partial^4 u}{\partial x^4}\\ &= \mu\frac{\partial^2}{\partial x^2}\left[\rho A(1+2v)\frac{\partial^2 u}{\partial t^2} - \rho I_p v^2\frac{\partial^4 u}{\partial x^2 \partial t^2} - \eta A\left(H_y^2 + H_z^2\right)\frac{\partial^2 u}{\partial x^2}\right]\end{aligned} \tag{26}$$

It should be noted that the magnetic-field-related higher-order term originates from the action of the differential nonlocal operator on the Lorentz force contribution appearing in Eq. (17).

3. Analytical solution

This section presents a step-by-step analytical solution of the governing equation for axial displacement $u(x,\ t)$ of nonlocal Bishop nanorod under effect of transverse magnetic field, based on harmonic motion assumption. The goal is to reduce the time-dependent partial differential equation (PDE) to an ordinary differential equation (ODE) dependent on the spatial variable and to obtain the natural frequency

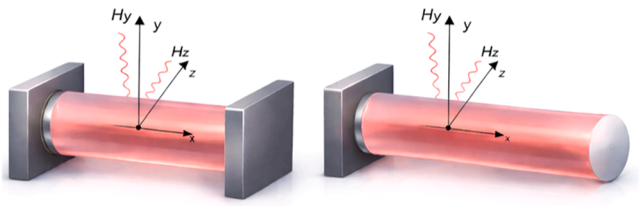


Fig. 2. Bishop nanorod's C-C and C-F boundary conditions.

equation along with the boundary conditions, so the following transformation is applied:

$$u(x,t) = U(x)e^{i\omega t} \tag{27}$$

where, $U(x)$ is the mode shape and ω is the natural frequency. The necessary derivatives with this transformation:

$$\frac{\partial^2 u}{\partial t^2} = -\omega^2 U(x)e^{i\omega t}, \frac{\partial^4 u}{\partial x^2 \partial t^2} = -\omega^2 U''(x)e^{i\omega t},$$

$$\frac{\partial^2 u}{\partial x^2} = U''(x)e^{i\omega t}, \frac{\partial^4 u}{\partial x^4} = U''(x)e^{i\omega t} \tag{28}$$

where, (') denotes x's derivative. When the above expressions are substituted into the Eq. (26) and common factor $e^{i\omega t}$ is simplified, a fourth-order ODE is obtained for $U(x)$:

$$A_4(\omega)U''(x) - A_2(\omega)U''(x) - A_0(\omega)U(x) = 0 \tag{29}$$

Here are the frequency-dependent coefficients:

$$A_4(\omega) = GI_p v^2 - \mu^2 \rho I_p v^2 \omega^2 + \mu^2 K_m \tag{30a}$$

$$A_2(\omega) = -\rho I_p v^2 \omega^2 + (EA + K_m) - \mu^2 \rho A(1+2v)\omega^2 \tag{30b}$$

$$A_0(\omega) = \rho A\omega^2 \tag{30c}$$

In the above equations, $K_m = \eta A\left(H_y^2 + H_z^2\right)$. Thus, Eq. (29) admits the following analytical solution:

$$U(x) = C_1\cos(\alpha x) + C_2\sin(\alpha x) + C_3\cosh(\beta x) + C_4\sinh(\beta x) \tag{31}$$

Here,

$$\alpha = \left(\frac{-A_2 + \sqrt{A_2^2 + 4A_4A_0}}{2A_4}\right)^{1/2}$$

$$\beta = \left(\frac{A_2 + \sqrt{A_2^2 + 4A_4A_0}}{2A_4}\right)^{1/2} \tag{32}$$

Additionally, $C_i\ (i = 1,2,3,4)$ denote unknown constants obtained with the relevant boundary conditions. As part of this study, the dynamic behavior of the Bishop nanorod was investigated under two different boundary conditions: clamped-clamped (C–C) and clamped-free (C–F, cantilever) configurations (Fig. 2).

First, local and nonlocal boundary conditions for the C–C configuration is given by:

$$U(0) = 0 \text{ and } \left(\mu^2\rho\omega^2 - G\right)U''(0) = 0$$

$$U(L) = 0 \text{ and } \left(\mu^2\rho\omega^2 - G\right)U''(L) = 0 \tag{33}$$

Using the above equation in Eq. (31), the solution can be written in matrix form:

$$\begin{bmatrix} 1 & 0 & 1 & 0 \\ -\xi\alpha^2 & 0 & \xi\beta^2 & 0 \\ \cos(\alpha L) & \sin(\alpha L) & \cosh(\beta L) & \sinh(\beta L) \\ -\xi\alpha^2\cos(\alpha L) & -\xi\alpha^2\sin(\alpha L) & \xi\beta^2\cosh(\beta L) & \xi\beta^2\sinh(\beta L) \end{bmatrix} \begin{bmatrix} C_1 \\ C_2 \\ C_3 \\ C_4 \end{bmatrix} = 0 \tag{34}$$

In the above equations, $\xi = \mu\rho\omega^2 - G$. Determinant of corresponding coefficient matrix must be zero to ensure a non-trivial solution, which leads to the following equation:

$$sin\ \alpha L = 0,\ \alpha = \frac{n\pi}{L}\ (n = 1, 2, ..) \tag{35}$$

Substituting Eq. (35) into Eq. (32), natural frequency of C-C nanorod is achieved as:

$$\omega_n = \sqrt{\frac{(GI_p v^2 + \mu^2 K_m)\left(\frac{n\pi}{L}\right)^4 + (EA + K_m)\left(\frac{n\pi}{L}\right)^2}{\mu^2\rho I_p v^2\left(\frac{n\pi}{L}\right)^4 + (\rho I_p v^2 + \mu^2\rho A(1+2v))\left(\frac{n\pi}{L}\right)^2 + \rho A}} \tag{36}$$

The local and nonlocal boundary conditions for C-F configuration is written as follows:

$$U(0) = 0 \text{ and } (\mu^2\rho\omega^2 - G)U''(0) = 0$$

$$\begin{aligned} U'(L) =& 0 \text{ and } \left(EA - \mu^2\rho A(1+2v)\omega^2 - \mu^2\eta A\left(H_y^2 + H_z^2\right)\right)U'(L) \\ & - v^2 I_p\left(G - \mu^2\rho\omega^2\right)U'''(L) = 0 \end{aligned} \tag{37}$$

Using the above equation in Eq. (31), the solution takes the following matrix form:

$$\begin{bmatrix} 1 & 0 & 1 & 0 \\ -\xi\alpha^2 & 0 & \xi\beta^2 & 0 \\ -\alpha\sin(\alpha L) & \alpha\cos(\alpha L) & \beta\sinh(\beta L) & \beta\cosh(\beta L) \\ -\xi v^2 I_p\alpha^3\sin(\alpha L) & \xi v^2 I_p\alpha^3\cos(\alpha L) & -\xi\beta^3\sinh(\beta L) & -\xi v^2 I_p\beta^3\cosh(\beta L) \end{bmatrix}$$

$$\begin{bmatrix} C_1 \\ C_2 \\ C_3 \\ C_4 \end{bmatrix} = 0 \tag{38}$$

Similarly, determinant of corresponding coefficient matrix must be zero to ensure a non-trivial solution, which leads to the following equation:

$$cos\ \alpha L = 0,\ \alpha = \frac{(2n-1)\pi}{2L}\ (n = 1, 2, ..) \tag{39}$$

Using Eq. (39) in Eq. (32), the natural frequency corresponding to the C–F nanorod is derived as:

$$\omega_n = \sqrt{\frac{(GI_p v^2 + \mu^2 K_m)\left(\frac{(2n-1)\pi}{2L}\right)^4 + (EA + K_m)\left(\frac{(2n-1)\pi}{2L}\right)^2}{\mu^2\rho I_p v^2\left(\frac{(2n-1)\pi}{2L}\right)^4 + (\rho I_p v^2 + \mu^2\rho A(1+2v))\left(\frac{(2n-1)\pi}{2L}\right)^2 + \rho A}} \tag{40}$$

When the magnetic field effect is neglected in Eqs. (36) and (40), the expression reduces to the Bishop nanorod model. Furthermore, when the lateral inertia effect and Poisson's ratio are also neglected, the resulting natural frequency equation transforms into the classical rod model.

4. Numerical results

The vibration response of Bishop nanorod subjected to magnetic field is analyzed in this study for two distinct boundary conditions. In the analysis, the nanorod length is considered as L = 20 nm with a circular cross-sectional diameter of d = 1 nm. Material properties are adopted from [70] as: $\rho = 2300 kg/m^3$, E = 1 TPa, $\upsilon = 0.19$, G = E /2(1 + υ) = 0.42 TPa.

Table 1
The first four dimensionless frequencies of Bishop nanorod ($K_m = 0$).

λ	Mode	C-F		C-C	
		Ref. [71]	This Study	Ref. [71]	This Study
0.0	1	1.57078	1.57074	3.14149	3.14119
	2	4.71205	4.71102	6.28237	6.27994
	3	7.85240	7.84765	9.42204	9.41386
	4	10.99123	10.97825	12.55989	12.54056
0.1	1	1.54471	1.54467	2.94720	2.94693
	2	4.12256	4.12176	5.05472	5.05309
	3	5.77150	5.76877	6.31589	6.31183
	4	6.72926	6.72367	7.04530	7.03797
0.2	1	1.47363	1.47360	2.52756	2.52736
	2	3.15845	3.15794	3.52357	3.52265
	3	3.74163	3.74019	3.87838	3.87634
	4	3.96836	3.96560	4.03013	4.02656

To derive dimensionless vibration frequencies, the following transformations are employed.

$$\lambda = \frac{\mu}{L},\ \overline{K_m} = \frac{K_m}{EA} = \gamma(1+\delta^2),\ \kappa = \frac{I_p}{AL^2},\ \frac{G}{E} \tag{41}$$

Additionally, magnetic parameter and magnetic field strengths' ratio are expressed as follows:

$$\gamma = \frac{\eta H_y^2}{E},\ \delta = \frac{H_z}{H_y} \tag{42}$$

Based on these formulations, the dimensionless frequencies the C–C and C–F boundary conditions are expressed as follows:

$$\overline{\omega}_n = \sqrt{\frac{\left(\frac{G}{E}\kappa v^2 + \lambda^2\overline{K_m}\right)\left(\frac{n\pi}{L}\right)^4 + (1+\overline{K_m})\left(\frac{n\pi}{L}\right)^2}{\lambda^2\kappa v^2\left(\frac{n\pi}{L}\right)^4 + \left(\kappa v^2 + \lambda^2(1+2v)\right)\left(\frac{n\pi}{L}\right)^2 + 1}} \tag{43}$$

$$\overline{\omega}_n = \sqrt{\frac{\left(\frac{G}{E}\kappa v^2 + \lambda^2\overline{K_m}\right)\left(\frac{(2n-1)\pi}{2L}\right)^4 + (1+\overline{K_m})\left(\frac{(2n-1)\pi}{2L}\right)^2}{\lambda^2\kappa v^2\left(\frac{(2n-1)\pi}{2L}\right)^4 + \left(\kappa v^2 + \lambda^2(1+2v)\right)\left(\frac{(2n-1)\pi}{2L}\right)^2 + 1}} \tag{44}$$

First, to verify the accuracy and consistency of proposed formulation, magnetic field effect was neglected; dimensionless and dimensional frequency values of Bishop nanorod were obtained for different nonlocal parameter values under C–F and C–C, and the obtained findings were compared with previous studies.

Subsequently, the model was reduced to a classical nanorod model by neglecting the effects of rotational inertia and shear stiffness considered within scope of the Bishop nanorod model, and results obtained in this case were compared with two different studies in the literature.

Table 2
Natural vibration frequencies (TPa) of Bishop nanorod according to various nonlocal parameter values ($K_m = 0$).

μ	C-F		C-C	
	Ref. [66]	This Study	Ref. [66]	This Study
0.0	1.72712	1.72707	3.45418	3.45378
0.2	1.72692	1.72687	3.45220	3.45220
0.4	1.72632	1.72628	3.44629	3.44748
0.6	1.72532	1.72529	3.43650	3.43965
0.8	1.72392	1.72391	3.42294	3.42877
1.0	1.72213	1.72215	3.40573	3.41494
1.2	1.71995	1.72000	3.38505	3.39826
1.4	1.71738	1.71747	3.36109	3.37886
1.6	1.71443	1.71456	3.33407	3.35689
1.8	1.71111	1.71128	3.30421	3.33249
2.0	1.70742	1.70765	3.45418	3.30585

Table 3
First four dimensionless frequencies values in classical nanorod ($K_m = 0$, $G = 0$, $I_p = 0$).

λ	Mode	C-F			C-C		
		This Study	Ref.[72]	Ref. [73]	This Study	Ref. [72]	Ref.[73]
0.0	1	1.57080	1.57080	1.57080	3.14159	3.14159	3.14159
	2	4.71239	4.71239	4.71239	6.28318	6.28319	6.28319
	3	7.85398	7.85398	7.85398	9.42477	9.42478	9.42478
	4	10.99557	10.99557	10.99557	12.56637	12.56637	12.56637
0.1	1	1.55177	1.55177	1.55177	2.99716	2.99717	2.99717
	2	4.26279	4.26279	4.26279	5.32018	5.32018	5.32018
	3	6.17668	6.17668	6.17668	6.85867	6.85867	6.85867
	4	7.39805	7.39805	7.39805	7.82479	7.82479	7.82479
0.2	1	1.49858	1.49858	1.49858	2.66009	2.66009	2.66009
	2	3.42933	3.42933	3.42933	3.91239	3.91239	3.91239
	3	4.21781	4.21782	4.21782	4.41692	4.41692	4.41692
	4	4.55152	4.55152	4.55152	4.64576	4.64576	4.64576

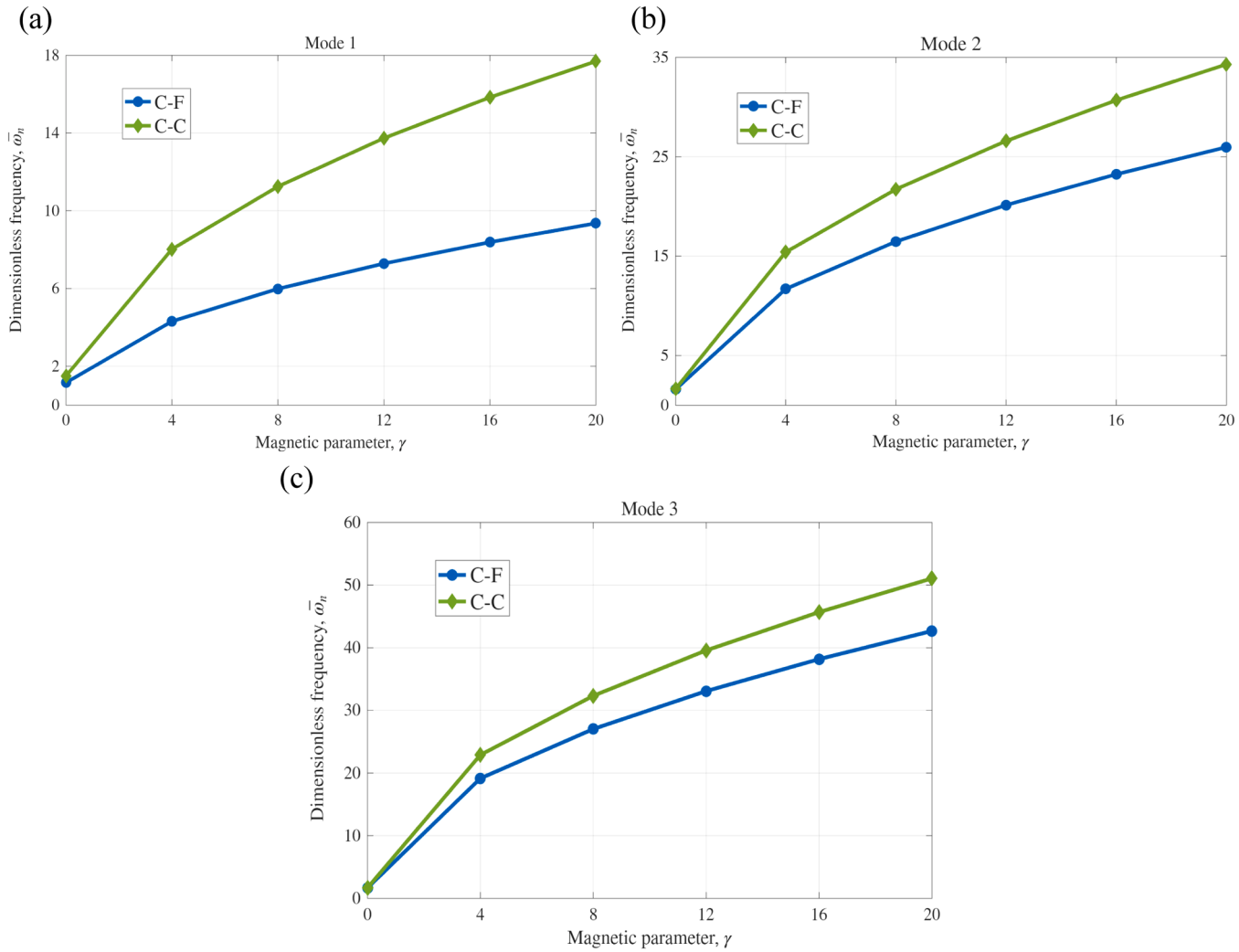


Fig. 3. Change in dimensionless natural frequency ($\bar{\omega}_n$) with the magnetic parameter (γ) (a) Mode 1, (b) Mode 2 and (c) Mode 3.

4.1. Validation studies

This study was compared with the reference study conducted by Ref. [71], neglecting effect of magnetic field. According to reference work, influence of the elastic medium was also considered as zero. In line with this approach, the dimensionless natural frequency values obtained by considering only the Bishop nanorod model are presented in Table 1 for the C-F and C-C.

Similarly, by neglecting the magnetic field parameters, the comparison of natural frequencies in the THz range obtained for different nonlocal parameter values within the Bishop nanorod model is presented in Table 2. In the computation of these values, the material and geometric parameters adopted in the reference study [66] were considered. Accordingly, the mass density was taken as L = 24.4 nm, E = 6.85 TPa and $\rho = 9517 \mathrm{kg/m^3}$.

The dimensionless natural frequency results obtained for the classical nanorod model, the magnetic field effect together with the

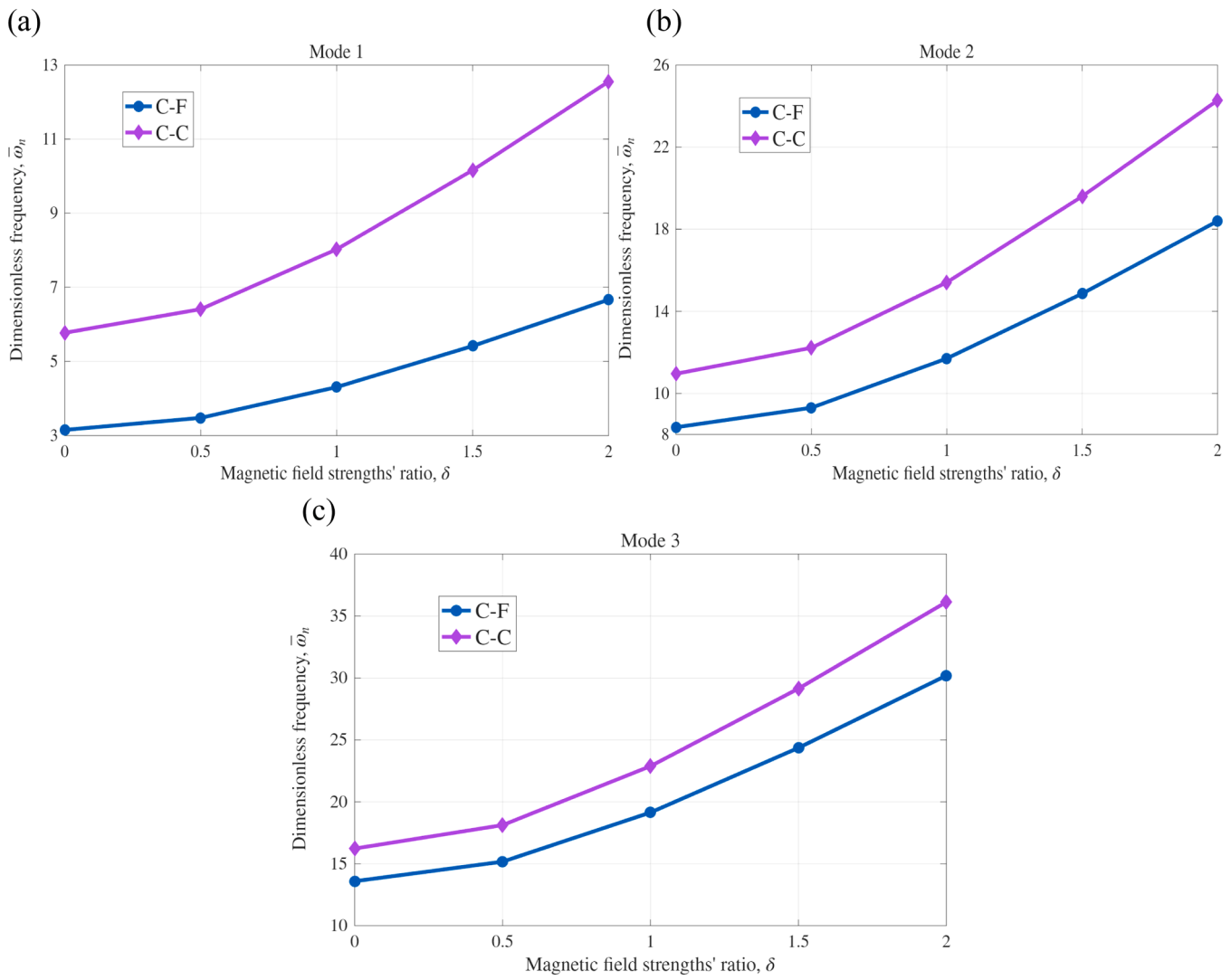


Fig. 4. Change in dimensionless natural frequency ($\overline{\omega}_n$) with the magnetic field strengths' ratio (δ) (a) Mode 1, (b) Mode 2 and (c) Mode 3.

rotational inertia and shear stiffness of the rod, are presented in Table 3 in comparison with two different studies [72,73].

Fig. 3 illustrates, for the first time, the role of the magnetic parameter on dimensionless frequencies of Bishop nanorod for three vibration modes. While obtaining the graphs, magnetic field strengths' ratio and dimensionless nonlocal parameter values were kept constant at $\delta = 1$ and $\lambda = 0.5$, respectively; the magnetic parameter (γ) was assumed to vary between 0 and 20. The findings show that increasing the magnetic parameter increases the system rigidity and consequently causes significant increase in the dimensionless frequencies. This reveals that magnetic field has a stiffening effect on structural behavior.

From a physical perspective, the increase in natural frequencies can be attributed to the additional repulsive force generated by the Lorentz interaction between the transverse magnetic field and the motion of the nanorod. As the magnetic parameter increases, the magnetic effect strengthens and creates additional resistance to deformation. Consequently, the effective stiffness of the system increases, leading to higher natural frequency values.

Additionally, natural frequencies are found to increase with higher mode numbers, while magnetic parameter enhances this increase under both boundary conditions.

The parameter δ used in the results presented in Fig. 4 is defined as the ratio of the component of the magnetic field in the z direction to its component in the y direction $(\delta = H_z/H_y)$. In this study, it was assumed that the parameter δ varies between 0 and 2. While obtaining the graphs, the magnetic parameter and the dimensionless nonlocal parameter values were kept constant at $\gamma = 4$ and $\lambda = 0.5$, respectively.

Increasing the δ parameter alters component distribution of the magnetic field within y–z plane, leading to an increase in magnetic energy contribution. This creates a stiffening effect on the axial vibration behavior. Consequently, an increase in δ parameter causes axial dimensionless natural frequencies in the x-direction to increase under two boundary conditions.

Figs. 5 and 6 illustrate how the nonlocal parameter affects the dimensionless natural frequencies of the classical and Bishop nanorod models under two boundary conditions. The effect of magnetic field was considered when obtaining graphs; magnetic parameter $\gamma = 4$ and the magnetic field strengths' ratio $\delta = 1$ were kept constant.

Examination of obtained results reveals that significant differences in frequency values arise between the classical and Bishop nanorod models as the nonlocal parameter increases. As the nonlocal parameter increases, the dimensionless natural frequencies decrease for both boundary conditions and for both rod models. This indicates that the nonlocal effect has a softening character in terms of system rigidity.

Furthermore, the Bishop rod model yields lower frequency values compared to the classical model because it considers rotational inertia effects and shear stiffness. This result demonstrates that inertia and shear effects should not be neglected in nanoscale structures.

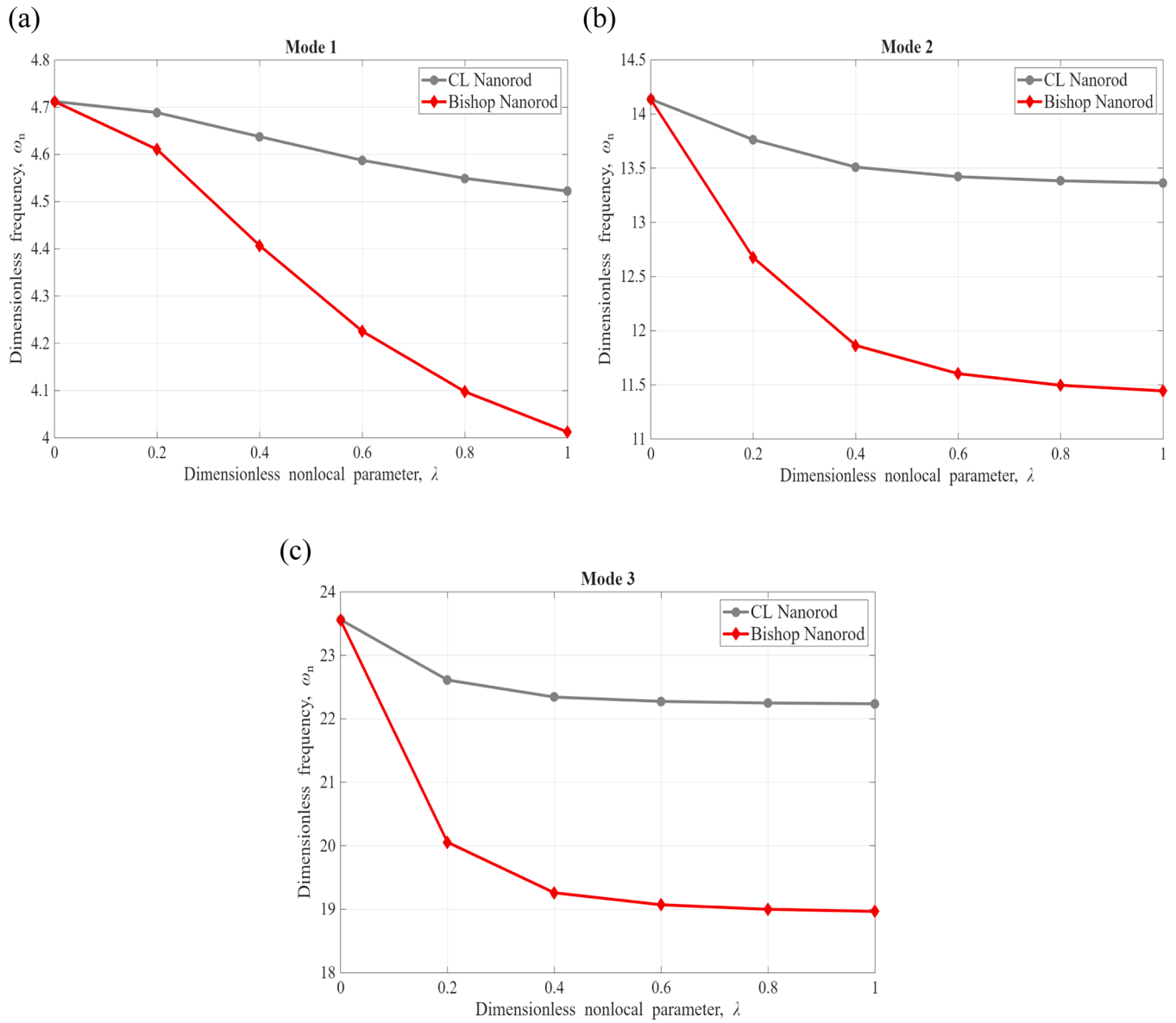


Fig. 5. Change in dimensionless natural frequency ($\overline{\omega}_n$) of classical and Bishop nanorods with dimensionless nonlocal parameter (λ) under C-F condition (a) Mode 1, (b) Mode 2 and (c) Mode 3.

To provide a direct assessment of the influence of lateral inertia and shear stiffness effects, Tablo 4 presents a quantitative comparison between the classical and Bishop nanorod models. The percentage difference is defined as:

$$\Delta(\%) = \frac{\overline{\omega}_{n,CL} - \overline{\omega}_{n,B}}{\overline{\omega}_{n,CL}} x100 \tag{45}$$

where $\overline{\omega}_{n,CL}$ and $\overline{\omega}_{n,B}$ denote the first dimensionless natural frequencies obtained from the classical and Bishop nanorod models, respectively. The percentage differences reported in the table clearly demonstrate the added value of the Bishop formulation in predicting the vibration response of nanorods subjected to magnetic fields (Table 4).

Tables 5 and 6 present dimensionless natural frequency values obtained for the first mode under two boundary conditions, in terms of nonlocal parameter, magnetic field parameter, and magnetic field strengths' ratio parameter.

Examination of the tables clearly indicates that, for both boundary conditions, increasing the parameters related to the magnetic field leads to higher natural frequency values. In contrast, natural frequencies exhibit a decreasing trend with increasing nonlocal parameter. This indicates that magnetic effect plays a stiffening role on the system, while the nonlocal effect plays a softening role.

The three-dimensional graphical representation of first three dimensionless natural frequencies, depending on nonlocal parameters, magnetic parameters, and magnetic field strength ratios, is presented in Fig. 7. Examination of the graphs reveals that the frequency values obtained under C–F are lower compared to C–C. This effect is related to the C–C boundary condition, meaning it provides higher rigidity and restricts the vibration behavior of the system more.

The resulting graphs clearly demonstrate the contrasting characteristics of the nonlocal softening effect and the magnetic hardening effect and show the decisive role of the interaction between parameters on the vibration behavior. Increasing the nonlocal parameter reduces the natural frequencies due to the weakening of the effective structural stiffness, whereas increasing the magnetic parameter and magnetic field strength ratio enhances the frequencies through the additional repulsive force generated by the magnetic field. Therefore, the vibration response of the nanorod is governed by the balance between these opposing

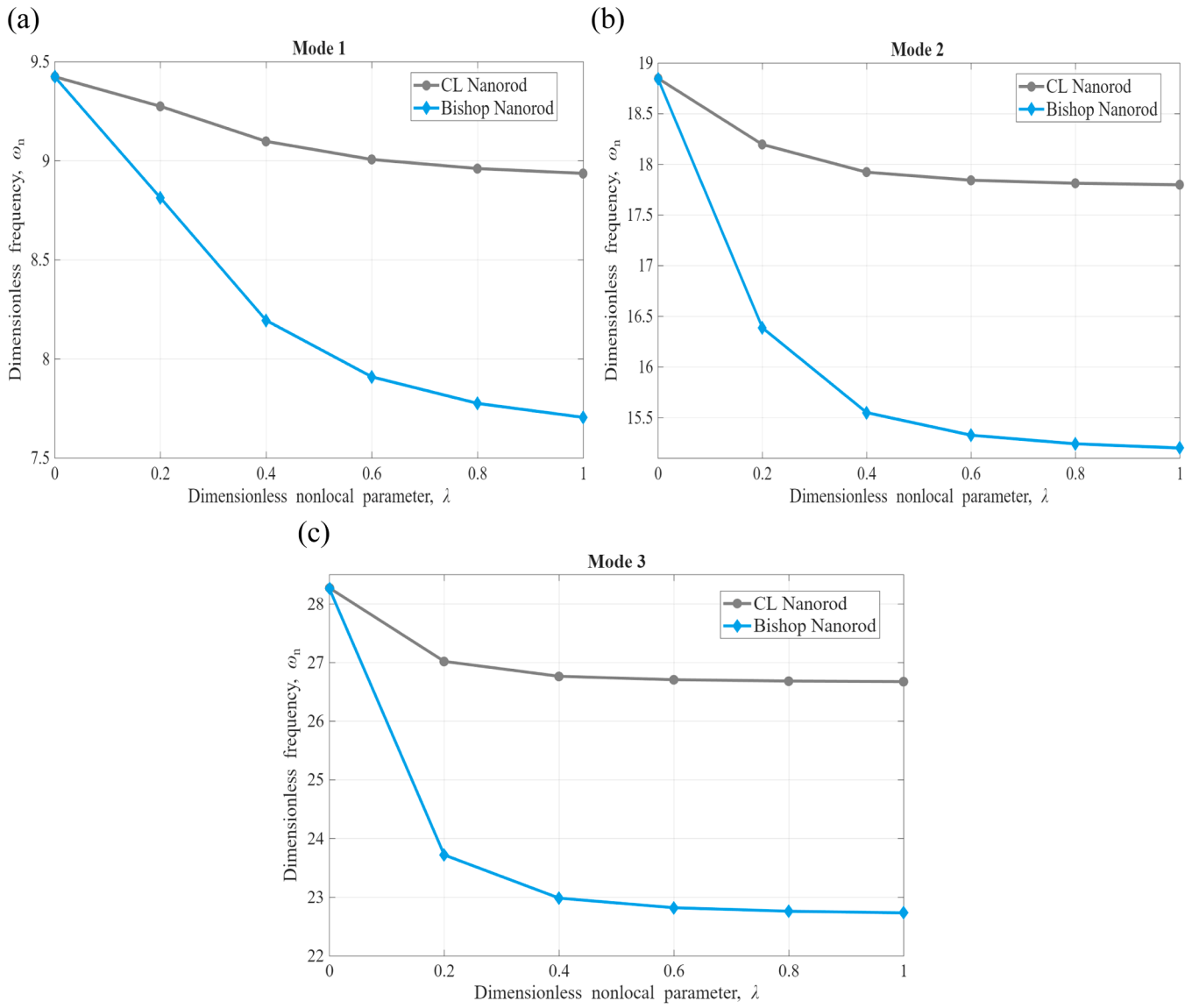


Fig. 6. Change in dimensionless natural frequency ($\overline{\omega}_n$) of classical and Bishop nanorods with dimensionless nonlocal parameter (λ) under C-C condition (a) Mode 1, (b) Mode 2 and (c) Mode 3.

Table 4
Percentage differences between the classical and Bishop nanorod models for the first dimensionless frequency ($\gamma = 4,\ \delta = 1$).

Boundary Condition	λ	$\overline{\omega}_{n,CL}$	$\overline{\omega}_{n,B}$	Δ(%)
C-F	0.0	4.7124	4.7123	0.00
	0.4	4.6377	4.4067	4.98
	0.8	4.5493	4.0975	9.93
C-C	0.0	9.4248	9.4243	0.01
	0.4	9.0985	8.1947	9.93
	0.8	8.9613	7.7758	13.23

Table 5
First dimensionless frequencies of Bishop nanorod for parameters λ, δ and γ under C-F boundary condition.

λ	δ	γ				
		4	8	12	16	20
0	0	3.5124	4.7124	5.6635	6.4765	7.1982
	0.5	3.8476	5.2097	6.2831	7.1982	8.0095
	1	4.7124	6.4765	7.8539	9.0235	10.0580
	2	7.1982	10.058	12.2680	14.1370	15.7860
0.5	0	3.1548	4.3096	5.2146	5.9843	6.6657
	0.5	3.4796	4.7835	5.8014	6.6657	7.4301
	1	4.3096	5.9843	7.2836	8.3839	9.3557
	2	6.6657	9.3557	11.429	13.181	14.725

mechanisms.

5. Conclusion

This study investigates, first analysis of longitudinal vibration behavior of a Bishop-type nanorod under a transverse magnetic field based on nonlocal elasticity theory. The equation of motion governing system is derived according to Bishop rod model, which incorporates both rotational inertia and shear deformation effects. Subsequently, the magnetic field contribution is introduced into the formulation through Maxwell's relations. By solving the resulting differential equations, analytical expressions for natural frequencies are obtained under two different boundary conditions, namely clamped–clamped and clamped–free. The accuracy and consistency of the model are verified by comparison with previous studies in the literature.

Table 6
The first dimensionless frequencies of Bishop nanorod for parameters λ, δ and γ under C-C boundary condition.

λ	δ	γ				
		4	8	12	16	20
0	0	7.0245	9.4243	11.327	12.952	14.396
	0.5	7.6949	10.419	12.566	14.396	16.018
	1	9.4243	12.952	15.707	18.046	20.115
	2	14.396	20.115	24.535	28.273	31.572
0.5	0	5.7718	8.0241	9.7703	11.249	12.554
	0.5	6.4095	8.9399	10.898	12.554	14.016
	1	8.0241	11.249	13.736	15.837	17.691
	2	12.554	17.691	21.641	24.974	27.912

Finally, an analysis of the natural frequency values is performed for various combinations of governing parameters under different boundary conditions. The key results of the study are summarized as follows:

- Increasing magnetic parameter leads to significant increase in natural frequency values under both boundary conditions. This is related to the magnetic field imparting additional effective rigidity to the system.
- Increasing in magnetic field strengths' ratios leads to significant increase in natural frequency values under both boundary conditions.
- Significant differences are observed between the vibration frequency values obtained from the classical nanorod model and Bishop nanorod model. This difference becomes even more pronounced when magnetic field and nonlocal parameter effects are considered. Furthermore, natural frequency values are reduced with increasing nonlocal parameter, which is related to the character of scale effects in reducing system rigidity.
- It was determined that the non-local parameter and the magnetic field parameter have opposite effects on the vibration frequency of the nanorod. The presence of magnetic field increases the natural frequency values, while an increase in the nonlocal parameter causes a decrease in frequency values.

This study presents a theoretical framework that can be used in the design and performance evaluation of nanoscale sensors, actuators, and NEMS-based devices operating under magnetic fields. Furthermore, the

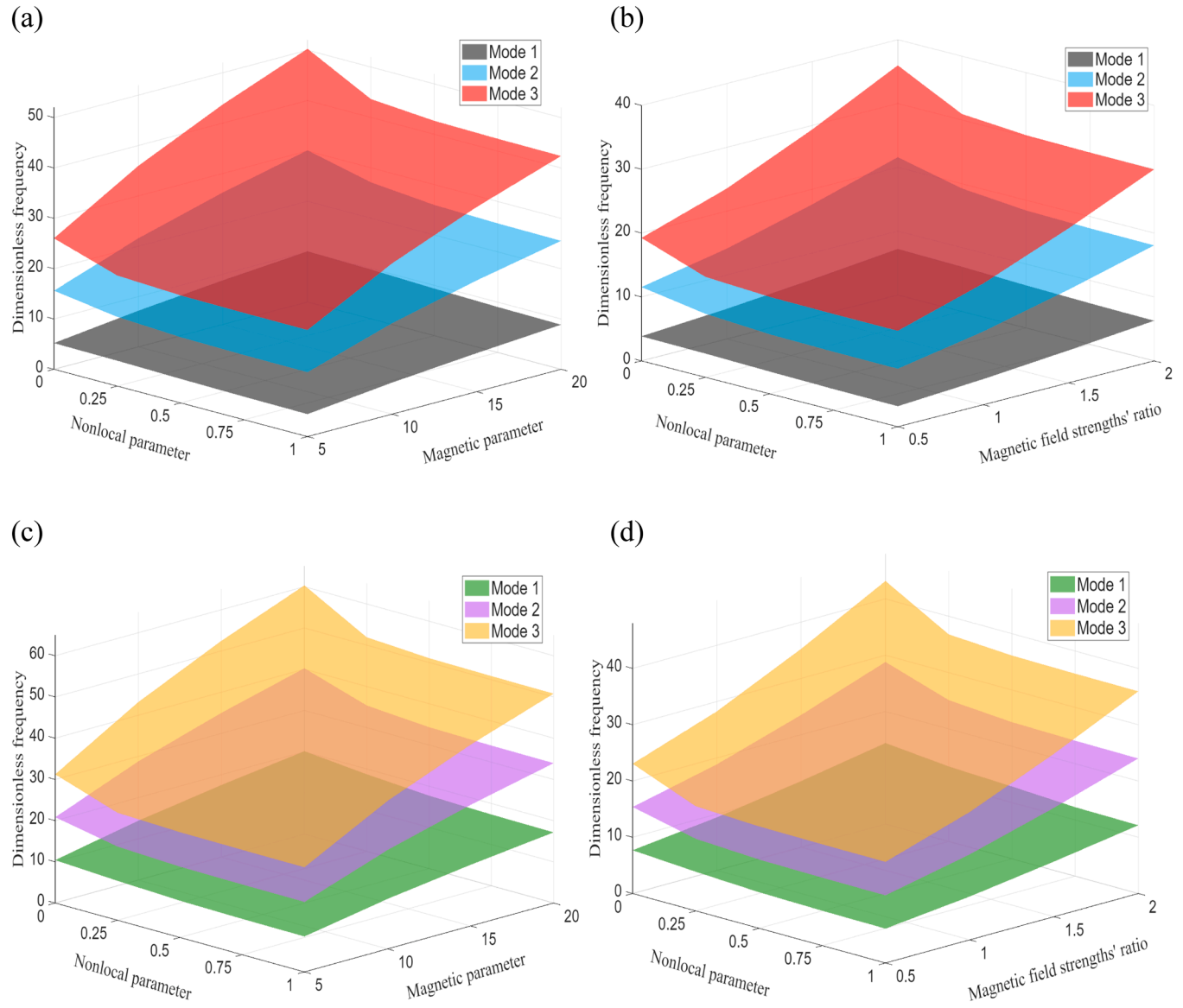


Fig. 7. Change in first three dimensionless natural frequencies with respect to nonlocal parameter, magnetic parameter, and magnetic field strength ratio (a-b) C-F and (c-d) C-C.

findings highlight the importance of using advanced Bishop type rod models in conjunction with nonlocal elasticity theory to accurately capture magnetic effects at the nanoscale. Another notable finding of this study is that the difference between the classical non-local rod model and the non-local Bishop rod model increases as the magnetic field strength increases. This behavior demonstrates that lateral inertia and shear stiffness effects become increasingly significant under magneto-elastic conditions and should therefore be considered in the dynamic analysis of nanorods.

Funding

No funding was received for conducting this study.

CRediT authorship contribution statement

Aleyna Yazıcıoğlu: Writing – original draft, Visualization, Software, Methodology, Investigation, Formal analysis, Data curation. **Ömer Civalek:** Writing – review & editing, Validation, Supervision, Methodology, Investigation, Conceptualization.

Declaration of competing interest

The authors declare that they have no known competing financial interests or personal relationships that could have appeared to influence the work reported in this paper.

Data availability

Data will be made available on request.

References

[1] K.S. Novoselov, A.K. Geim, S.V. Morozov, D. Jiang, Y. Zhang, S.V. Dubonos, I. V. Grigorieva, A.A. Firsov, Electric field in atomically thin carbon films, Science 306 (2004) 666–669, https://doi.org/10.1126/science.1102896.
[2] A. Javey, J. Guo, Q. Wang, M. Lundstrom, H. Dai, Ballistic carbon nanotube field-effect transistors, Nature 424 (2003) 654–657, https://doi.org/10.1038/nature01797.
[3] C.K. Chan, H. Peng, G. Liu, K. McIlwrath, X.F. Zhang, R.A. Huggins, Y. Cui, High-performance lithium battery anodes using silicon nanowires, Nat. Nanotechnol. 3 (2007) 31–35, https://doi.org/10.1038/nnano.2007.411.
[4] R.H. Baughman, C. Cui, A.A. Zakhidov, Z. Iqbal, J.N. Barisci, G.M. Spinks, G. G. Wallace, A. Mazzoldi, D. De Rossi, A.G. Rinzler, O. Jaschinski, S. Roth, M. Kertesz, Carbon nanotube actuators, Science 284 (1999) 1340–1344, https://doi.org/10.1126/science.284.5418.1340.
[5] O.C. Farokhzad, R. Langer, Nanomedicine: developing smarter therapeutic and diagnostic modalities, Adv. Drug Deliv. Rev. 58 (2006) 1456–1459, https://doi.org/10.1016/j.addr.2006.09.011.
[6] F. Sanchez, K. Sobolev, Nanotechnology in concrete: a review, Constr. Build. Mater. 24 (2010) 2060–2071, https://doi.org/10.1016/j.conbuildmat.2010.03.014.
[7] A.C. Eringen, On differential equations of nonlocal elasticity and solutions of screw dislocation and surface waves, J. Appl. Phys. 54 (1983) 4703–4710, https://doi.org/10.1063/1.332803.
[8] A.C. Eringen, D.G.B. Edelen, On nonlocal elasticity, Int. J. Eng. Sci. 10 (1972) 233–248, https://doi.org/10.1016/0020-7225(72)90039-0.
[9] F. Yang, A.C.M. Chong, D.C.C. Lam, P. Tong, Couple stress based strain gradient theory for elasticity, Int. J. Solids Struct. 39 (2002) 2731–2743, https://doi.org/10.1016/S0020-7683(02)00152-X.
[10] D.C.C. Lam, F. Yang, A.C.M. Chong, J. Wang, P. Tong, Experiments and theory in strain gradient elasticity, J. Mech. Phys. Solids 51 (2003) 1477–1508, https://doi.org/10.1016/S0022-5096(03)00053-X.
[11] M.E. Gurtin, A.I. Murdoch, A continuum theory of elastic material surfaces, Arch. Ration. Mech. Anal. 57 (1975) 291–323, https://doi.org/10.1007/BF00261375.
[12] M. Ferrari, T.G. Vladimir, A. Imam, J.C. Nadeau, Advances in Doublet Mechanics, Springer Science & Business Media, 2008.
[13] C.W. Lim, G. Zhang, J.N. Reddy, A higher-order nonlocal elasticity and strain gradient theory and its applications in wave propagation, J. Mech. Phys. Solids 78 (2015) 298–313, https://doi.org/10.1016/j.jmps.2015.02.001.
[14] E. Benvenuti, A. Simone, One-dimensional nonlocal and gradient elasticity: closed-form solution and size effect, Mech. Res. Commun. 48 (2013) 46–51, https://doi.org/10.1016/j.mechrescom.2012.12.001.
[15] N. Challamel, C.M. Wang, The small length scale effect for a non-local cantilever beam: a paradox solved, Nanotechnology 19 (2008) 345703, https://doi.org/10.1088/0957-4484/19/34/345703.
[16] P.L. Bian, H. Qing, C.F. Gao, One-dimensional stress-driven nonlocal integral model with bi-Helmholtz kernel: close form solution and consistent size effect, Appl. Math. Model. 89 (2021) 400–412, https://doi.org/10.1016/J.APM.2020.07.058.
[17] P. Zhang, H. Qing, Two-phase nonlocal integral models with a bi-Helmholtz averaging kernel for nanorods, Appl. Math. Mech. 42 (2021) 1379–1396, https://doi.org/10.1007/S10483-021-2774-9.
[18] P. Zhang, H. Qing, Thermoelastic analysis of nanobar based on nonlocal integral elasticity and nonlocal integral heat conduction, J. Therm. Stresses. 44 (2021) 1244–1261, https://doi.org/10.1080/01495739.2021.1967240.
[19] H. Song, H. Qing, Static extension and vibration analysis of piezoelectric semiconductor nanobars based on two-phase local/nonlocal integral models, Acta Mech. 237 (2025) 299–315, https://doi.org/10.1007/S00707-025-04535-Y.
[20] J. Peddieson, G.R. Buchanan, R.P. McNitt, Application of nonlocal continuum models to nanotechnology, Int. J. Eng. Sci. 41 (2003) 305–312, https://doi.org/10.1016/S0020-7225(02)00210-0.
[21] J.N. Reddy, Nonlocal theories for bending, buckling and vibration of beams, Int. J. Eng. Sci. 45 (2007) 288–307, https://doi.org/10.1016/J.IJENGSCI.2007.04.004.
[22] H.T. Thai, A nonlocal beam theory for bending, buckling, and vibration of nanobeams, Int. J. Eng. Sci. 52 (2012) 56–64, https://doi.org/10.1016/J.IJENGSCI.2011.11.011.
[23] Ç. Demir, Ö. Civalek, On the analysis of microbeams, Int. J. Eng. Sci. 121 (2017) 14–33, https://doi.org/10.1016/J.IJENGSCI.2017.08.016.
[24] B. Akgöz, Ö. Civalek, Strain gradient elasticity and modified couple stress models for buckling analysis of axially loaded micro-scaled beams, Int. J. Eng. Sci. 49 (2011) 1268–1280, https://doi.org/10.1016/j.ijengsci.2010.12.009.
[25] S. Adhikari, D. Gilchrist, T. Murmu, M.A. McCarthy, Nonlocal normal modes in nanoscale dynamical systems, Mech. Syst. Signal Process. 60–61 (2015) 583–603, https://doi.org/10.1016/j.ymssp.2014.12.004.
[26] M.A. Eltaher, S.A. Emam, F.F. Mahmoud, Free vibration analysis of functionally graded size-dependent nanobeams, Appl. Math. Comput. 218 (2012) 7406–7420, https://doi.org/10.1016/J.AMC.2011.12.090.
[27] F. Ebrahimi, E. Salari, Thermal buckling and free vibration analysis of size dependent Timoshenko FG nanobeams in thermal environments, Compos. Struct. 128 (2015) 363–380, https://doi.org/10.1016/j.compstruct.2015.03.023.
[28] I. Elishakoff, J. Kaplunov, E. Nolde, Celebrating the centenary of Timoshenko's study of effects of shear deformation and rotary inertia, Appl. Mech. Rev. 67 (2015), https://doi.org/10.1115/1.4031965.
[29] R. Barretta, L. Feo, R. Luciano, F. Marotti de Sciarra, A gradient Eringen model for functionally graded nanorods, Compos. Struct. 131 (2015) 1124–1131, https://doi.org/10.1016/j.compstruct.2015.06.077.
[30] M. Aydogdu, M. Arda, Forced vibration of nanorods using nonlocal elasticity, Adv. Nano Res. 4 (2016) 265–279, https://doi.org/10.12989/anr.2016.4.4.265.
[31] R. Nazemnezhad, K. Kamali, An analytical study on the size dependent longitudinal vibration analysis of thick nanorods, Mater. Res. Express. 5 (2018) 075016, https://doi.org/10.1088/2053-1591/AACF6E.
[32] R. Nazemnezhad, K. Kamali, Free axial vibration analysis of axially functionally graded thick nanorods using nonlocal Bishop's theory, Steel Compos. Struct. 28 (2018) 749–758, https://doi.org/10.12989/SCS.2018.28.6.749.
[33] M. Arda, J. Majak, M. Mehrparvar, Longitudinal wave propagation in axially graded Rayleigh–Bishop nanorods, Mech. Compos. Mater. 59 (2024) 1109–1128, https://doi.org/10.1007/S11029-023-10160-4.
[34] F.P. Pinnola, R. Luciano, F. Marotti de Sciarra, Static analysis of porous Bishop nanorods embedded in an elastic medium, Compos. Struct. 387 (2026) 120332, https://doi.org/10.1016/J.COMPSTRUCT.2026.120332.
[35] R. Barretta, S.A. Faghidian, F. Marotti de Sciarra, A consistent variational formulation of Bishop nonlocal rods, Contin. Mech. Thermodyn. 32 (2020) 1311–1323, https://doi.org/10.1007/S00161-019-00843-6.
[36] X.F. Li, Z.B. Shen, K.Y. Lee, Axial wave propagation and vibration of nonlocal nanorods with radial deformation and inertia, Z. Angew. Math. Mech. 97 (2017) 602–616, https://doi.org/10.1002/ZAMM.201500186.
[37] M. Arda, Axial dynamics of functionally graded Rayleigh–Bishop nanorods, Microsyst. Technol. 27 (2021) 269–282, https://doi.org/10.1007/S00542-020-04950-2.
[38] U. Gul, M. Aydogdu, Longitudinal vibration of Bishop nanorods model based on nonlocal strain gradient theory, J. Braz. Soc. Mech. Sci. Eng. 44 (2022) 377, https://doi.org/10.1007/S40430-022-03635-3.
[39] S.J. Shakhlavi, R. Nazemnezhad, Comprehensive study of internal modal interactions: comparison of various axial nonlinear beam theories, Adv. Nano Res. 16 (2024) 273–288, https://doi.org/10.12989/ANR.2024.16.3.273.
[40] M. Ghadiri, H. Hajbarati, M. Safi, Vibration analysis of single-walled carbon peapods based on nonlocal Timoshenko beam theory, Appl. Phys. A Mater. Sci. Process. 123 (2017) 260, https://doi.org/10.1007/s00339-017-0811-y.
[41] R. Ansari, M. Faraji Oskouie, S. Nesarhosseini, H. Rouhi, Flexoelectricity effect on the size-dependent bending of piezoelectric nanobeams resting on elastic foundation, Appl. Phys. A Mater. Sci. Process. 127 (2021) 518, https://doi.org/10.1007/s00339-021-04654-y.
[42] H.M. Numanoğlu, Ö. Civalek, On the torsional vibration of nanorods surrounded by elastic matrix via nonlocal FEM, Int. J. Mech. Sci. 161–162 (2019) 105076, https://doi.org/10.1016/j.ijmecsci.2019.105076.
[43] M.A. Alazwari, I. Esen, A.A. Abdelrahman, A.M. Abdraboh, M.A. Eltaher, Dynamic analysis of functionally graded (FG) nonlocal strain gradient nanobeams under thermo-magnetic fields and moving load, Adv. Nano Res. 12 (2022) 231–251, https://doi.org/10.12989/anr.2022.12.3.231.

[44] A. Seyfi, A. Teimouri, F. Ebrahimi, Scale-dependent torsional vibration response of non-circular nanoscale auxetic rods, Waves Random Complex. Media. 34 (2024) 4425–4441, https://doi.org/10.1080/17455030.2021.1990441.
[45] X. Yan, Free vibration analysis of a rotating nanobeam using integral form of Eringen's nonlocal theory and element-free Galerkin method, Appl. Phys. A Mater. Sci. Process. 128 (2022) 641, https://doi.org/10.1007/s00339-022-05714-7.
[46] Ö. Civalek, M. Şeker, H.M. Numanoğlu, In-plane free vibration analysis of nonlocal nanorings embedded in elastic medium, Appl. Phys. A Mater. Sci. Process. 131 (2025) 69, https://doi.org/10.1007/s00339-024-08204-0.
[47] B. Uzun, U. Kafkas, B. Deliktaş, M.Ö. Yaylı, Size-dependent vibration of porous Bishop nanorod with arbitrary boundary conditions and nonlocal elasticity effects, J. Vib. Eng. Technol. 11 (2022) 809–826, https://doi.org/10.1007/s42417-022-00610-z.
[48] M. Simyari, S.A. Hosseini, Analytical solution for nonlocal forced vibration of elliptical nanorod under linear and nonlinear external torque, Appl. Math. Model. 124 (2023) 353–366, https://doi.org/10.1016/j.apm.2023.07.022.
[49] M.S. Taima, T.A. El-Sayed, M.I. Friswell, Thermal vibration analysis of cracked nanobeams submerged in elastic foundations by nonlocal continuum mechanics, Thin-Walled Struct. 193 (2023) 111249, https://doi.org/10.1016/j.tws.2023.111249.
[50] M. Zarepour, S.B. Choi, Analytical modeling and simulations of a piezoelectric nanorod for energy harvesting via Eringen's differential model, Appl. Phys. A Mater. Sci. Process. 130 (2024) 749, https://doi.org/10.1007/s00339-024-07896-8.
[51] R. Nazemnezhad, R. Ashrafian, Free transverse vibration analysis of spinning Timoshenko–Ehrenfest nano-beams through two-phase local/nonlocal elasticity theory, Appl. Phys. A Mater. Sci. Process. 130 (2024) 199, https://doi.org/10.1007/s00339-024-07350-9.
[52] A.E. Abouelregal, B. Akgöz, Ö. Civalek, Nonlocal thermoelastic vibration of a solid medium subjected to a pulsed heat flux via Caputo–Fabrizio fractional derivative heat conduction, Appl. Phys. A Mater. Sci. Process. 128 (2022) 660, https://doi.org/10.1007/s00339-022-05786-5.
[53] A. Yazıcıoglu, O. Civalek, Free axial and torsional vibration of boron nitride nanorods using nonlocal finite element method, J. Comput. Appl. Mech. 57 (2026) 107–121, https://doi.org/10.22059/JCAMECH.2025.403575.1634.
[54] T. Murmu, S. Adhikari, M.A. McCarthy, Axial vibration of embedded nanorods under transverse magnetic field effects via nonlocal elastic continuum theory, J. Comput. Theor. Nanosci. 11 (2014) 1230–1236, https://doi.org/10.1166/jctn.2014.3487.
[55] D. Karličic, M. Cajić, T. Murmu, P. Kozić, S. Adhikari, Nonlocal effects on the longitudinal vibration of a complex multi-nanorod system subjected to the transverse magnetic field, Meccanica 50 (2015) 1605–1621, https://doi.org/10.1007/s11012-015-0111-6.
[56] K. Kiani, Vibration and instability of a single-walled carbon nanotube in a three-dimensional magnetic field, J. Phys. Chem. Solids 75 (2014) 15–22, https://doi.org/10.1016/j.jpcs.2013.07.022.
[57] K. Kiani, Magnetically affected single-walled carbon nanotubes as nanosensors, Mech. Res. Commun. 60 (2014) 33–39, https://doi.org/10.1016/j.mechrescom.2014.05.005.
[58] K. Kiani, Longitudinally varying magnetic field influenced transverse vibration of embedded double-walled carbon nanotubes, Int. J. Mech. Sci. 87 (2014) 179–199, https://doi.org/10.1016/j.ijmecsci.2014.04.018.
[59] S. Narendar, S.S. Gupta, S. Gopalakrishnan, Wave propagation in single-walled carbon nanotube under longitudinal magnetic field using nonlocal Euler–Bernoulli beam theory, Appl. Math. Model. 36 (2012) 4529–4538, https://doi.org/10.1016/j.apm.2011.11.073.
[60] K. Kiani, Elastic wave propagation in magnetically affected double-walled carbon nanotubes, Meccanica 4 (50) (2014) 1003–1026, https://doi.org/10.1007/s11012-014-9957-2.
[61] A.G. Arani, M.H. Jalaei, Investigation of the longitudinal magnetic field effect on dynamic response of viscoelastic graphene sheet based on sinusoidal shear deformation theory, Physica B Condens. Matter. 506 (2017) 94–104.
[62] R. Özmen, R. Kılıç, I. Esen, Thermomechanical vibration and buckling response of nonlocal strain gradient porous FG nanobeams subjected to magnetic and thermal fields, Mech. Adv. Mater. Struct. 31 (2024) 834–853, https://doi.org/10.1080/15376494.2022.2124000.
[63] B. Uzun, Magnetic field and non-local effects on axial vibration of embedded nanorods reinforced with short fibers, Acta Mech. 236 (2025) 4889–4920, https://doi.org/10.1007/s00707-025-04417-3.
[64] Y. Zhou, Y.F. Zheng, F. Wang, C.P. Chen, Size-dependent nonlinear free vibration of magneto-electro-elastic nanobeams by incorporating modified couple stress and nonlocal elasticity theory, Phys. Scr. 99 (2024) 095217, https://doi.org/10.1088/1402-4896/AD67B6.
[65] I. Ahmadi, M. Najafi, V. Sladek, J. Sladek, Free vibration analysis of magneto-electro-elastic nanobeams in flexural and thickness modes, J. Braz. Soc. Mech. Sci. Eng. 48 (2025), https://doi.org/10.1007/S40430-025-05935-W.
[66] D.Z. Karličić, S. Ayed, E. Flaieh, Nonlocal axial vibration of the multiple Bishop nanorod system, Math. Mech. Solids 24 (2019) 1668–1691, https://doi.org/10.1177/1081286518766577.
[67] J.N. Reddy, Energy Principles and Variational Methods in Applied Mechanics, John Wiley & Sons, 2002. Incorporated.
[68] A.G. Arani, E. Haghparast, H.B. Zarei, Nonlocal vibration of axially moving graphene sheet resting on orthotropic visco-Pasternak foundation under longitudinal magnetic field, Physica B Condens. Matter. 495 (2016) 35–49, https://doi.org/10.1016/j.physb.2016.04.039.
[69] D. Karličić, P. Kozić, S. Adhikari, M. Cajić, T. Murmu, M. Lazarević, Nonlocal mass-nanosensor model based on the damped vibration of single-layer graphene sheet influenced by in-plane magnetic field, Int. J. Mech. Sci. 96–97 (2015) 132–142, https://doi.org/10.1016/j.ijmecsci.2015.03.014.
[70] J.N. Reddy, S.D. Pang, Nonlocal continuum theories of beams for the analysis of carbon nanotubes, J. Appl. Phys. 103 (2008), https://doi.org/10.1063/1.2833431.
[71] Ö. Civalek, H.M. Numanoğlu, Nonlocal finite element analysis for axial vibration of embedded love–bishop nanorods, Int. J. Mech. Sci. 188 (2020) 105939, https://doi.org/10.1016/j.ijmecsci.2020.105939.
[72] H.M. Numanoğlu, B. Akgöz, Ö. Civalek, On dynamic analysis of nanorods, Int. J. Eng. Sci. 130 (2018) 33–50, https://doi.org/10.1016/j.ijengsci.2018.05.001.
[73] X.J. Xu, M.L. Zheng, X.C. Wang, On vibrations of nonlocal rods: boundary conditions, exact solutions and their asymptotics, Int. J. Eng. Sci. 119 (2017) 217–231, https://doi.org/10.1016/j.ijengsci.2017.06.025.